Inorganic Chemistry

Article

pubs.acs.org/IC

Solvothermal Synthesis and Characterization of a Series of Lanthanide Thiostannates(IV): The First Examples of Inorganic–Organic Hybrid Cationic Lanthanide Thiostannates(IV)

Jian Zhou,*,[†,§] Xing Liu,[†] Litao An,[‡] Feilong Hu,[†] Wenbin Yan,[§] and Yunyan Zhang[†]

[†]College of Chemistry and Material, Yulin Normal University, Yulin 537000, P.R. China

[‡]Jiangsu Key Laboratory for Chemistry of Low-Dimensional Materials, College of Chemistry and Chemical Engineering, Huaiyin Normal University, Huaian, 223300, P.R. China

[§]College of Chemistry and Chemical Engineering, Jishou University, Jishou, 416000, P.R. China

S *Supporting Information*

ABSTRACT: A series of new lanthanide thiostannates(IV), $[Y_2(dien)_4(\mu\text{-}OH)_2]Sn_2S_6$ (**1**, dien = diethyl-enetriamine), $(tetaH)_2[Ln_2(teta)_2(tren)_2(\mu\text{-}Sn_2S_6)]Sn_2S_6$ [*Ln* = Eu (**2**), Sm (**3**); teta = triethylenetetramine; tren = tris(2-aminoethyl)amine] and $[Eu_2(tepa)_2(\mu\text{-}OH)_2(\mu\text{-}Sn_2S_6)]\text{-}(tepa)_{0.5}\cdot H_2O$ (**4**, tepa = tetraethylene-pentamine) were solvothermally synthesized and structurally characterized. **1** consists of a binuclear $[Y_2(dien)_4(\mu_2\text{-}OH)_2]^{4+}$ cation and a discrete dimeric $[Sn_2S_6]^{4-}$ anion. Both **2** and **3** are isostructural and composed of $[Ln_2(teta)_2(tren)_2(\mu\text{-}Sn_2S_6)]^{2+}$ cations, protonated triethylenetetramines (tetaH), and discrete dimeric $[Sn_2S_6]^{4-}$ anions. A $Sn_2S_6{}^{4-}$ anion bridges two $[Ln(teta)(tren)]^{3+}$ cations via the *trans*-S_t (*t* = terminal) atoms to form the first examples of inorganic−organic hybrid thiostannate cations $[Ln_2(teta)_2(tren)_2(\mu\text{-}Sn_2S_6)]^{2+}$. **4** consists of one-dimensional (1-D) neutral chains $[Eu_2(tepa)_2(\mu\text{-}OH)_2(\mu\text{-}Sn_2S_6)]_n$ built up from the linkage of dinuclear complex cations $[Eu_2(tepa)_2(\mu_2\text{-}OH)_2]^{4+}$ and bridging anions $[Sn_2S_6]^{4-}$, free tepa molecules, and lattice water molecules. The present compounds exhibit wide-band gap semiconducting properties with absorption band edges between 2.40 and 2.91 eV.

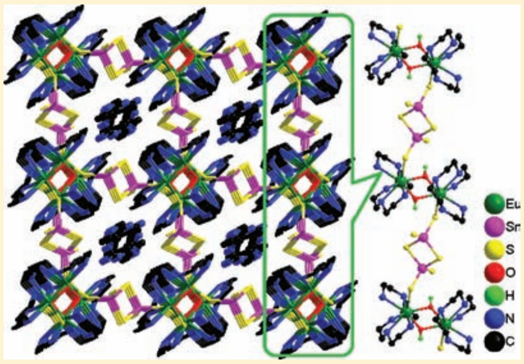

■ INTRODUCTION

The incorporation of metal complexes (MCs) into the main-group metal chalcogenide framework has been extensively studied because it may generate a variety of previously unseen architectures with potential applications in semiconductors, photoluminescence, magnetic materials, ferroelectricity, nonlinear optics, and so forth.[1] The very important aspect is that the integration of the electronic, optical, and magnetic properties of MCs with the host inorganic chalcogenidometalate framework can be expected to provide complementary properties and synergistic effects. In the case of chalcogenidostannate, the vast majority of solvothermal reactions carried out in the presence of transition-metal (*TM*) ions lead to the formation of anionic chalcogenidostannate frameworks charge-balanced by isolated transition-metal complex cations (TMCs), where the coordination sphere of *TM* ions is completed by three bidentate or two tridentate chelating amines.[2] But there have been relatively few reports of the incorporation of TMCs into the chalcogenidostannate frameworks. Substantial success has recently been achieved with chalcogenidostannate by using a tetradentate (teta and tren) or pentadentate (tepa) chelating amine, which coordinates to the *TM* ion with at least one coordination site of the *TM* atom in favor of further bonding with the Q atoms of the $Sn_xQ_y{}^{n-}$ (Q = S, Se, Te) units, the limited examples include $[TM(tren)]_2(\mu_2\text{-}Sn_2S_6)$ (*TM* = Co, Ni),[2a] $[Mn(tren)]_2(\mu_2\text{-}Sn_2Se_6)$,[3] $[TM(tepa)]_2(\mu_2\text{-}Sn_2Q_6)$ (*TM* = Mn, Fe, Co; Q = S, Se),[4] $\{[Mn(teta)]_2SnS_4\}\cdot 4H_2O$,[5] $[Mn(tepa)\cdot Sn_3Se_7]_n$,[4a] and $[Mn(teta)(en)]\cdot[Mn(teta)]\text{-}[Mn(SnTe_4)_2\cdot Mn(teta)]$.[1d] Applying Mn, Zn, Cu, Ag, or Hg, it is not necessary to use such multidentate amines, evidenced by $(1,4\text{-}dabH)_2MnSnS_4$,[6] $(dienH_2)Cu_2Sn_2S_6$,[7] $(1,4\text{-}dabH_2)\text{-}Cu_2SnS_4$,[8] $(1,4\text{-}dabH_2)Ag_2SnS_4$,[9] $(enH_2)HgSnS_4$,[10] $[\{Mn(en)_2\}_2(\mu_2\text{-}en)(\mu_2\text{-}Sn_2S_6)]_n$,[11] $[\{Mn(terpy)\}_2(\mu_2\text{-}Sn_2Se_6)]_n$,[11] $[\{Mn(cyclam)\}_2(\mu_2\text{-}Sn_2Se_{6.15})]$,[12] $(ape)_2Zn_2Sn_2Se_7$ (ape = *N*-(2-aminoethyl)piperazine),[1h] and $[Zn(H_2O)_4]\text{-}[Zn_2Sn_3Se_9(MeNH_2)]$,[1g] However, compared with chalcogenidostannates combined with TMCs, the chalcogenidostannates with lanthanide(III) complexes are less explored under mild solvothermal conditions.[13] Moreover, all of these compounds contain either chalcogenidostannate anions or neutral organic hybrid chalcogenidostannates with negative charged cores, but cationic organic hybrid chalcogenidostannates have not been reported until now.

Multinary lanthanide chalcogenides are of great interest in solid-state chemistry because of their promising applications in

Received: October 25, 2011
Published: January 26, 2012

dx.doi.org/10.1021/ic2023083 | *Inorg. Chem.* 2012, 51, 2283−2290

Table 1. Crystallographic Data for 1−4

	1	2	3	4
formula	$C_{16}H_{54}N_{12}O_2S_6Sn_2Y_2$	$C_{36}H_{110}Eu_2N_{24}S_{12}Sn_4$	$C_{36}H_{110}N_{24}S_{12}Sm_2Sn_4$	$C_{20}H_{61.5}Eu_2N_{12.5}O_3S_6Sn_2$
Fw	1054.37	2042.83	2039.63	1258.98
crystal system	monoclinic	triclinic	triclinic	monoclinic
space group	$P2_1/n$	$P\bar{1}$	$P\bar{1}$	$C2/c$
a, Å	11.854(8)	9.886(2)	9.920(2)	19.803(4)
b, Å	11.449(7)	10.371(2)	10.382(2)	14.998(3)
c, Å	13.803(9)	17.442(4)	17.520(4)	17.800(4)
α, deg	90	89.78(3)	89.91(3)	90
β, deg	97.978(9)	88.00(3)	88.07(3)	126.57(3)
γ, deg	90	85.14(3)	85.23(3)	90
V, Å^3	1855(2)	1780.8(6)	1797.1(7)	4246(2)
Z	2	1	1	4
T, K	296(2)	296(2)	296(2)	296(2)
calcd density, Mg m^{-3}	1.888	1.898	1.877	1.970
abs coeff, mm^{-1}	4.800	3.514	3.371	4.411
$F(000)$	1048	1004	1002	2460
2θ(max), deg	50.18	50.20	50.20	52.20
total reflns collected	9636	9519	9771	12024
unique reflns	3306	6206	6292	4192
no. of param	181	362	362	239
$R1[I > 2\sigma(I)]$	0.0441	0.0999	0.0290	0.0540
$wR2$(all data)	0.1133	0.2867	0.0878	0.1782
GOF on F^2	1.011	1.006	1.076	1.048

optical fibers, doped semiconductors, and nanocluster fluorescence labels.[14] These materials are usually made by flux methods at high temperature, such as $Eu_5Sn_3S_{12}$,[15] $EuCu_2SnS_4$,[16] and $Ln_2Mn_3Sb_4S_{12}$ (Ln = Pr, Nd, Sm, Gd).[17] However, the synthesis of lanthanide chalcogenides modified with organic components remains a big challenge because they are comparatively unstable with respect to heat, water, oxygen, and light.[18] Moreover, these soft Lewis basic Q^{2-} ligands (Q = S, Se, Te) coordinate with difficulty to the hard Lewis acidic lanthanide(III) ions (Ln^{3+}) via Ln−Q bonds in the solvents. More recently, we have attempted the preparation of lanthanide chalcogenides in chelating amine solutions by the solvothermal methods, and prepared two organic hybrid lanthanide thioantimonates, [Eu(dien)$_2$SbS$_3$] and {[Eu(dien)$_2$]$_2$(μ_4-Sb$_2$S$_5$)}Cl$_2$,[19] which are rare examples of the [Sb^{III}S$_3$] unit as an unusual chelating ligand to a lanthanide complex. To obtain the analogous lanthanoide thiostannates, we started to explore the Sn/Ln_2O_3/S/amine system (amine = organic chelating amine) under solvothermal conditions, and successfully synthesized a series of lanthanide thiostannates(IV), [Y$_2$(dien)$_4$(μ-OH)$_2$]Sn$_2$S$_6$ (**1**), (tetaH)$_2$[Ln_2(teta)$_2$(tren)$_2$(μ-Sn$_2$S$_6$)]Sn$_2$S$_6$ [Ln = Eu (**2**), Sm (**3**)], and [Eu$_2$(tepa)$_2$(μ-OH)$_2$(μ-Sn$_2$S$_6$)](tepa)$_{0.5}$·H$_2$O (**4**). Although a few lanthanide thiostannates under solvothermal conditions have been reported,[13d,e] thiostannates mainly occurs as an isolated [Sn$_2$S$_6$]$^{4-}$ anion with a saturated lanthanide complex as counterion. The [Sn$_2$S$_6$]$^{4-}$ anion as a bridging ligand in compounds **2**−**4** connects the lanthanide complex cations to form the first inorganic−organic hybrid thiostannate cations {[Ln_2(teta)$_2$(tren)$_2$(μ-Sn$_2$S$_6$)]$^{2+}$} and a rare one-dimensional (1-D) organic hybrid Eu−S−Sn chain {[Eu$_2$(tepa)$_2$(μ-OH)$_2$(μ-Sn$_2$S$_6$)]}.

■ EXPERIMENTAL SECTION

General Remarks. All analytical grade chemicals were obtained commercially and used without further purification. Elemental analyses (C, H, and N) were performed using a PE2400 II elemental analyzer. The UV/vis spectra were recorded at room temperature using a computer-controlled PE Lambda 900 UV/vis spectrometer equipped with an integrating sphere in the wavelength range of 250−800 nm. FT-IR spectra were recorded with a Nicolet Magna-IR 550 spectrometer in dry KBr disks in the 4000−400 cm^{-1} range. Fluorescence spectral analyses were performed using a Cary Eclips fluorescence spectrometer. Thermogravimetric analyses (TGA) were performed using a Mettler TGA/SDTA851 thermal analyzer under a N$_2$ atmosphere with a heating rate of 10 °C min^{-1} in the temperature region of 25−500 °C. Compounds **1**−**4** are unstable to the moisture and air.

Synthesis of Lanthanide Thiostannates(IV). *Synthesis of [Y$_2$(dien)$_4$(μ-OH)$_2$]Sn$_2$S$_6$ (1).* The reagents of Sn (0.0098 g, 0.08 mmol), S (0.0198 g, 0.62 mmol), Y$_2$O$_3$ (0.0098 g, 0.04 mmol), and dien (2 mL) were placed in a thick Pyrex tube (ca. 20 cm long). The sealed tube was heated at 160 °C for 8 days to yield light yellow block-shaped crystals. The crystals were washed with ethanol, dried, and stored under vacuum (61% yield based on Sn). Elemental analysis. Found: C 18.19%, H 5.23%, N 15.88%; calcd C 18.23%, H 5.16%, N 15.94%. IR (cm^{-1}): 3362(s), 3178(s), 2929(s), 2857(s), 1576(s), 1498(s), 1392(m), 1326(m), 1071(m), 998(m), 954(m), 887(w), 809(w), 765(vw), 676(w), 616(m), 493(w), 460(m), 399(w).

Synthesis of (tetaH)$_2$[Eu$_2$(teta)$_2$(tren)$_2$(μ-Sn$_2$S$_6$)]Sn$_2$S$_6$(2). The reagents of Sn (0.0124 g, 0.10 mmol), S (0.0198 g, 0.62 mmol), Eu$_2$O$_3$ (0.0118 g, 0.03 mmol), and teta (2 mL) were placed in a thick Pyrex tube (ca. 20 cm long). The sealed tube was heated at 160 °C for 10 days to yield light yellow block-shaped crystals. The crystals were washed with ethanol, dried, and stored under vacuum (53% yield based on Sn). Elemental analysis. Found: C 21.11%, H 5.50%, N 16.41%; calcd C 21.17%, H 5.43%, N 16.46%. IR (cm^{-1}): 3180(s), 3085(s), 2913(s), 2863(s), 1576(m), 1503(m), 1459(m), 1375(w), 1320(m), 1076(s), 1020(w), 959(s), 887(w), 809(w), 737(vw), 666(w), 599(w), 471(m).

Synthesis of (tetaH)$_2$[Sm$_2$(teta)$_2$(tren)$_2$(μ-Sn$_2$S$_6$)]Sn$_2$S$_6$ (3). The light yellow crystals of (tetaH)$_2$[Sm$_2$(teta)$_2$(tren)$_2$(μ-Sn$_2$S$_6$)]Sn$_2$S$_6$ (**3**) were prepared by a similar method used in the synthesis of the crystals of **2** except that Eu$_2$O$_3$ was replaced by Sm$_2$O$_3$ (45% yield based on Sn). Elemental analysis. Found: C 21.13%, H 5.51%, N 16.42%; calcd C 21.20%, H 5.44%, N 16.48%. IR (cm^{-1}): 3179(s), 3079(s), 2913(s),

Table 2. Ranges of Some Important Bond Lengths (Å) and Angles (deg) for **1**−**4**[a]

		1	
Sn1−S_t	2.3338(19)−2.3497(18)	Sn1−S_b	2.4540(18)−2.4871(18)
Y1−N	2.498(5)−2.593(5)	Y1−O	2.221(4)−2.270(4)
S−Sn1−S	91.61(6)−118.61(6)	O−Y1−O	67.55(16)
O−Y1−N	74.71(15)−151.45(16)	N−Y1−N	66.87(16)−148.14(17)
		2	
Sn1−S_t	2.310(5)	Sn1−S_b	2.432(5)−2.447(5)
Sn1−S(−Ln)	2.360(5)	Sn2−S_t	2.329(6)−2.330(5)
Sn2−S_b	2.435(6)−2.455(6)	Eu1−S	2.939(4)
Eu1−N	2.544(18)−2.741(19)	N−Eu1−S	72.1(4)−143.8(5)
N−Eu1−N	65.5(6)−145.0(6)	S−Sn2−S	92.08(19)−113.98(19)
S−Sn1−S	92.08(19)−124.2(4)		
		3	
Sn1−S_t	2.3265(14)	Sn1−S_b	2.4404(15)−2.4540(14)
Sn1−S(−Ln)	2.3479(14)	Sn2−S_t	2.3345(16)−2.3428(14)
Sn2−S_b	2.4517(15)−2.4729(16)	Sm1−S	2.9637(15)
Sm1−N	2.567(4)−2.755(5)	N−Sm1−S	72.19(11)−144.01(15)
N2−Sm1−N	65.13(15)−145.29(14)	S−Sn2−S	92.47(5)−114.11(6)
S−Sn1−S	93.77(5)−116.90(5)		
		4	
Sn1−S_t	2.347(4)	Sn1−S_b	2.442(4)−2.449(4)
Sn1−S(−Ln)	2.343(3)	Eu1−O1	2.292(8)−2.340(8)
Eu1−S2	2.878(3)	Eu1−N5	2.585(11)−2.617(13)
O−Eu1−O	70.8(3)	O−Eu1−N	76.5(3)−151.3(3)
N−Eu1−N1	65.7(4)−141.0(4)	O−Eu1−S	80.7(2)−100.1(2)
N−Eu1−S	74.8(3)−154.3(3)	S−Sn1−S	93.34(11)−117.57(13)

[a] t = terminal, b = bridging.

2863(s), 1570(s), 1509(m), 1448(s), 1381(w), 1326(m), 1076(s), 1021(m), 993(m), 959(m), 876(w), 809(w), 738(vw), 654(vw), 604(w), 532(vw), 488(m).

Synthesis of $[Eu_2(tepa)_2(\mu\text{-}OH)_2(\mu\text{-}Sn_2S_6)](tepa)_{0.5}\cdot(H_2O)$ *(4).* The colorless crystals of $[Eu_2(tepa)_2(\mu\text{-}OH)_2(\mu\text{-}Sn_2S_6)](tepa)_{0.5}\cdot(H_2O)$ (**4**) were prepared by a similar method used in the synthesis of the crystals of **2** except that teta was replaced by tepa (72% yield based on Sn). Elemental analysis. Found: C 19.01%, H 5.05%, N 13.88%; calcd C 19.08%, H 4.92%, N 13.91%. IR (cm^{-1}): 3329(s), 3140(s), 2901(s), 2863(s), 1586(m), 1465(m), 1392(w), 1309(w), 1282(vw), 1092(m), 1059(m), 1020(m), 948(s), 904(w), 865(w), 827(w), 765(w), 571(w), 482(w), 422(m).

Crystal Structure Determination. Single-crystal X-ray diffraction data for **1**−**4** were recorded on a Rigaku Mercury CCD diffractometer using an ω-scan method with graphite monochromated Mo Kα radiation (λ = 0.71073 Å) at 296(2) K to a maximum 2θ value (52.20°). Absorption corrections were applied using the multiscan technique. The structures of **1**−**4** were solved by Direct Methods (SHELXS-97)[20] and refined by full-matrix least-squares techniques using the SHELXL-97 program.[21] Non-hydrogen atoms were refined with anisotropic displacement parameters. The H atoms bonded to C and N atoms were positioned with idealized geometry and refined with fixed isotropic displacement parameters, while the H atoms of C13 and N9 atoms were not dealt with because of the disorder of N9 atoms for **2** and **3**. For **4**, SIMU restraint prevents all adjacent C/N atoms to adopt different orientations. The N9 atoms for **2** and **3** were disordered over site occupation factors 0.53/0.47 and 0.50/0.50, respectively. The site occupation factors of N6, N7−N8, C9−C12, and O2 atoms for **4** were 0.50/0.50. The *wR*2 values for **2** and **4** are slightly large, which could be due to some disorder in the organic amines, but this could not be resolved. Relevant crystal and collection data parameters and refinement results can be found in Table 1. Additional details of crystal data in CIF format can be found in the Supporting Information. Ranges of some important bond lengths and angles for **1**−**4** are listed in Table 2. The CCDC reference numbers for **1**−**4** are 848791−848794, respectively.

■ RESULTS AND DISCUSSION

Description of the Structures. *Dimeric* $[Sn_2S_6]^{4-}$ *Anions.* The dimeric $[Sn_2S_6]^{4-}$ anions in compounds **1**−**4** are formed by two SnS_4 tetrahedra sharing a common edge. In **1**, the $[Sn_2S_6]^{4-}$ anion is discrete, while in **2**−**4**, the $[Sn_2S_6]^{4-}$ anions act as bidentate bridging ligands linking coordinatively unsaturated lanthanide complex cations, where the interatomic distances and angles are in the typical range of those for the well-known discrete $[Sn_2S_6]^{4-}$ or bridging $[\mu\text{-}Sn_2S_6]^{4-}$ anions reported in the literature.[2−5,11] The discrete $[Sn_2S_6]^{4-}$ anions exhibit crystallographic C_i symmetry, but bridging $[\mu\text{-}Sn_2S_6]^{4-}$ anions display very approximately C_{2h} symmetry. Because of S-Ln coordination, the ideal C_{2h} symmetry will be reduced owing to differences in the Sn−S(t) and Sn−S(−Ln) bond distances (Table 2).

Dimeric $[Sn_2S_6]^{4-}$ *Anion with Saturated Binuclear Complex Cation.* Single crystals of $[Y_2(dien)_4(\mu\text{-}OH)_2]Sn_2S_6$ (**1**) are obtained by the reaction of Sn, S, Y_2O_3, and dien under mild solvothermal conditions. **1** crystallizes in the monoclinic space group $P2_1/n$ with two formula units in the unit cell. **1** is composed of a discrete dimeric $[Sn_2S_6]^{4-}$ anion and a charge compensating binuclear complex cation $[Y_2(dien)_4(\mu_2\text{-}OH)_2]^{4+}$ (Figure 1a). Each Y^{3+} ion is in a bicapped trigonal prism by coordinating to six N atoms of two dien ligands and two −OH groups. Two $[Y(dien)_2]^{3+}$ moieties are joined by two μ_2-OH bridging groups to give a centrosymmetric dinuclear complex cation, where a Y_2O_2 rhomboidal core is formed. The Y1···Y1 separation is 3.733(2) Å, which is slightly longer than that in $Y(tpy)(OH)_2Br_3\cdot6H_2O$ (3.673 Å, tpy = 2,2′:6′,2″-terpyridine)[22] and $[Y(OH)(H_2O)_2(phen)_2]_2Cl_4\cdot2(phen)\cdot MeOH$ (3.651 Å, phen = 1,10-phenanthroline).[23] The Y−O (2.221(4)−2.270(4) Å) and Y−N (2.498(5)−2.593(5) Å) bond lengths are slightly shorter than those reported for $[Ln_2(en)_6(\mu\text{-}OH)_2]Sn_2S_6$ (Ln =

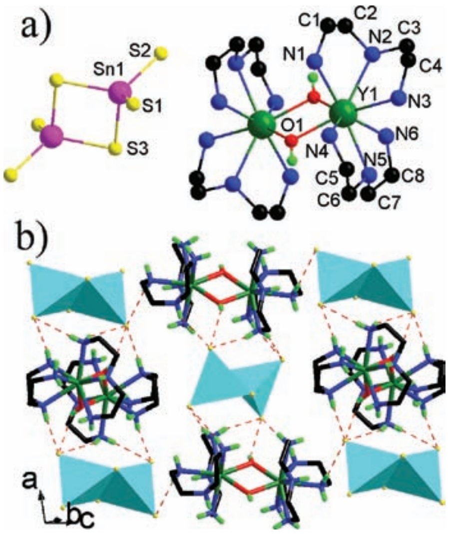

Figure 1. (a) Crystal structure of **1** [The H atoms bonded to C and N atoms are omitted for clarity]. (b) Part of the crystal structure of **1**, showing the formation of a (010) sheet constructed from N−H···S and O−H···S H-bonds [Blue tetrahedral: $[Sn_2S_6]^{4-}$ anion].

Nd, Gd)[13d] and $[Ln_2(en)_6(\mu\text{-}OH)_2]Sn_2Se_6$ (Ln = Pr, Nd, Gd),[13c] which is in agreement with the smaller radius of Y^{3+} compared to other Ln^{3+}. All S atoms of $[Sn_2S_6]^{4-}$ are involved in intermolecular N−H···S and N−H···O H-bonding interactions with $[Y_2(dien)_4(\mu_2\text{-}OH)_2]^{4+}$ cations leading to a layered arrangement parallel to the (010) plane (Figure 1b). The layers interact also via similar H-bonds resulting in a three-dimensional (3-D) H-bonding network structure (Supporting Information, Figure S1). The N···S distances vary from 3.431(5) to 3.713(5) Å and the N−H···S angles vary from 141.6 to 169.7°. The O···S distance is 3.237(4) Å and the O−H···S angle is 127.9°. These values are consistent with those reported in the literature.[13d,e]

Covalently Linked Complex Cations and Dimeric $[Sn_2S_6]^{4-}$ Anions Showing Variable Structures. Tetra- or pentadentate chelating amines have been used to form complex cations with unsaturated coordination spheres, which are able to be further coordinated by the chalcogenidometalate anion and act as structure modifying moieties/bridging nodes.[2a,3−5] Guided by this idea, we have successfully obtained two new types of thiostannates (IV) incorporated with lanthanide complexes, $(tetaH)_2[Ln_2(teta)_2(tren)_2(\mu\text{-}Sn_2S_6)][Sn_2S_6]$ (Ln = Eu (**2**), Sm (**3**)) and $[Eu_2(tepa)_2(\mu\text{-}OH)_2(\mu\text{-}Sn_2S_6)](tepa)_{0.5}\cdot H_2O$ (**4**) by replacing dien with teta or tepa under mild solvothermal conditions. Both **2** and **3** are isostructural and crystallize in the triclinic centrosymmetric space group $P\bar{1}$. Hence, only **2** is discussed here in detail. **2** consists of $[Eu_2(teta)_2(tren)_2(\mu\text{-}Sn_2S_6)]^{2+}$ cations, protonated triethylenetetramines (tetaH), and discrete dimeric $[Sn_2S_6]^{4-}$ anions (Figure 2a). In the $[Eu_2(teta)_2(tren)_2(\mu\text{-}Sn_2S_6)]^{2+}$ cation, $Sn_2S_6^{\ 4-}$ anion bridges two $[Eu(teta)(tren)]^{3+}$ cations via the *trans*-S_t (t = terminal) atoms to form a $[Eu_2(teta)_2(tren)_2(\mu\text{-}Sn_2S_6)]^{2+}$ cation with the Eu···Eu distance being 12.119 Å. The tren molecules in **2** and **3** must be from the solvent teta, since commercial teta is not an absolute reagent. Each Eu^{3+} ion is in a 9-fold coordination of eight N atoms from one teta and one tren molecule, and one S atom from a dimeric $[Sn_2S_6]^{4-}$ anion, yielding a distorted monocapped square antiprism. The Eu−N bond lengths are within the normal range. The Eu−S (2.939(4) Å) bond length is slightly longer than that reported for $[Eu(dien)_2SbS_3]$ (2.782(2)−2.838(2) Å) and $\{[Eu(dien)_2]_2(\mu_4\text{-}Sb_2S_5)\}Cl_2$ (2.785(3)−2.859(3) Å),[19] which may be caused by the higher coordination number of 9 (8N + 1S) of the Eu atom.

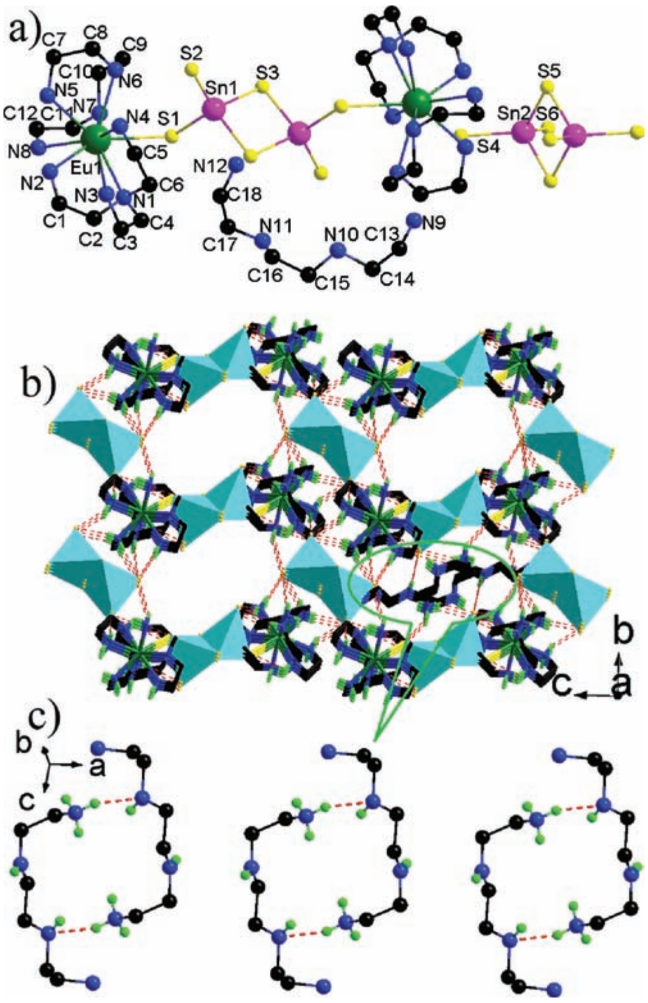

Figure 2. (a) Crystal structure of **2**, the H atoms bonded to C and N atoms are omitted for clarity. (b) 3-D H-bonding network structure in **2**, showing 1-D centrosymmetric elliptical channels [Blue tetrahedral: $[Sn_2S_6]^{4-}$ anion]. (c) dimeric $(tetaH)_2$ units with $R^2_2(16)$ ring arranged along the [100] direction.

The $[Eu_2(teta)_2(tren)_2(\mu\text{-}Sn_2S_6)]^{2+}$ cations in **2** are arranged in a dumbbell-like manner along the *a* and *c* axis, forming a pseudolayer within the (010) plane. The orientation of adjacent pseudolayers is identical, and the stacking sequence can be described as −AAA− fashion. The discrete dimeric $[Sn_2S_6]^{4-}$ anions are sandwiched between the pseudolayers and form extensive N−H···S H-bonds with the N atoms of the pseudolayer. The interconnection of the pseudolayers with discrete $[Sn_2S_6]^{4-}$ anions via H-bonds gives a 3-D H-bonding network structure with 1-D centrosymmetric elliptical channels along the [100] direction (Figure 2b). Two teta molecules interact via N−H···N H-bonds generating a dimeric $(tetaH)_2$ unit as new structure-directing agents (Figure 2c), exhibiting a centrosymmetric elliptical $R^2_2(16)$ ring[24] being located in the 1-D channel. These rings are arranged along the 1-D channel to form a 1-D centrosymmetric elliptical pseudochannel. The configuration of the pseudochannel shows a good match with that of the channel, suggesting that the guest $(tetaH)_2$ structure-directing agents can impose its individual configuration constraint on the host framework via N−H⋯S H-bonding interactions.[25]

Interestingly, the reported chalcogenidostannates(IV) covalently linked with metal complex cations are usually anions, $[Cr(en)_2(SnSe_4)]^-$,[26] and $[Ln(dien)_2(\mu\text{-}SnSe_4)]^-$ (Ln = Sm, Eu),[13c] neutral molecules, $[TM(tren)]_2(\mu_2\text{-}Sn_2S_6)$ (TM = Co, Ni),[2a] $[Mn(tren)]_2(\mu_2\text{-}Sn_2Se_6)$,[3] and $[TM(tepa)]_2(\mu_2\text{-}Sn_2Q_6)$ (TM = Mn, Fe, Co; Q = S, Se),[4] 1-D neutrally polymeric chains, $[\{Mn(en)_2\}_2(\mu\text{-}en)(\mu\text{-}Sn_2S_6)]$,[11] $\{[Mn(teta)]_2SnS_4\}\cdot 4H_2O$,[5] $[\{Mn(terpy)\}_2(Sn_2Se_6)]$,[12] $[Mn(tepa)\cdot Sn_3Se_7]$,[4a] $[Mn(teta)(en)]\cdot[Mn(teta)][Mn(SnTe_4)_2\cdot Mn(teta)]$,[1d] or two-dimensional (2-D) neutral layer, $(ape)_2Zn_2Sn_2Se_7$,[1h] but no cationic organic hybrid chalcogenidostannates (IV) have been reported until now. Hence, $[Ln_2(teta)_2(tren)_2(\mu\text{-}Sn_2S_6)]^{2+}$ (Ln = Eu, Sm) cations in **2** and **3** represent a new structural motif. Moreover, other cationic chalcogenidometalates are very scarce, and appear to be limited to those of $[In(en)_2Q]_2\cdot 2I$ (Q = Se, Te),[27] $[In(teta)Q]_2\cdot 2I$ (Q = Se, Te),[27] $[\{In(dien)\}_2(InTe_4)]\cdot Cl$,[27a] $\{[In(C_6H_{14}N_2)_2]_2Sb_4S_8\}Cl_2$,[28] and $\{[Eu(dien)_2]_2(\mu_4\text{-}Sb_2S_5)\}\text{-}Cl_2$,[19] where the counterions are halogen ions Cl^- and I^-. However, no coexistence of an organic hybrid chalcogenidometalate cation and discrete chalcogenidometalate anion was observed prior to this work. Therefore, both **2** and **3** possessing $[Ln_2(teta)_2(tren)_2(\mu\text{-}Sn_2S_6)]^{2+}$ (Ln = Eu, Sm) cations and discrete dimeric $[Sn_2S_6]^{4-}$ anions as counterions provide a new type.

The crystal structure of **4** is significantly different from that of **2** and **3**, which could result from different organic amines (teta for **2** and **3**, and tepa for **4**) directing the formation of the different structures. **4** crystallizes in the monoclinic centrosymmetric space group $C2/c$ and consists of 1-D $[Eu_2(tepa)_2(\mu\text{-}OH)_2(\mu\text{-}Sn_2S_6)]_n$ neutral chains, free tepa molecules, and lattice water molecules (Figure 3a). There is one unique Eu^{3+} ion in the asymmetric unit. The Eu^{3+} ion is in a distorted bicapped trigonal prism, which is formed by five N atoms of one tepa ligand, two O atoms of −OH groups, and one S atom of one $[Sn_2S_6]^{4-}$ anion. Two [Eu(tepa)] moieties are joined by two μ_2-OH bridging groups to give a coordinatively unsaturated centrosymmetric dinuclear cation $[Eu_2(tepa)_2(\mu_2\text{-}OH)_2]^{4+}$ with the Eu⋯Eu separation of 3.7761(17) Å. The Eu−N bond lengths vary from 2.585(11) to 2.617(13) Å and the Eu−O bond lengths are in the range from 2.292(8) to 2.340(8) Å, which are in the normal range. The Eu−S bond length of 2.878(3) Å is slightly shorter than that for **2**, whose longer distance can mainly be ascribed to the higher coordination number of 9 (8N + 1S) of the Eu atom in **2** as opposed to 8 (5N + 2O + 1S) in **4**.

Notably, the coordinatively unsaturated dinuclear lanthanide complex as bridging nodes within the chalcogenidometalates of the group 13−15 elements is uncommon, and normally they occur mononuclear.[13a,b,29] For instance, the 1-D La−Sb−S chain, $[La(en)_3(\mu_3\text{-}SbS_4)]_n$,[29b] is formed by the interconnection of $[La(en)_3]^{3+}$ complexes and multidentate $[SbS_4]$ bridging units. The 1-D La−Sn−Se chain in $[\{La(dien)_2\}_4(\mu_4\text{-}Sn_2Se_9)(\mu\text{-}Sn_2Se_6)]_n$,[13a] is constructed by the linkage of $\{La(dien)_2\}^{3+}$ complex, $[Sn_2Se_9]$ and $[Sn_2Se_6]$ units. The 1-D La−As−Se chain in $[La(en)_3(H_2O)(AsSe_4)]_n$[29d] is built up from $[Ln(en)_3(H_2O)]^{3+}$ complexes and bidentate $[AsSe_4]$ bridging units. Moreover, the reported dinuclear lanthanide complexes are generally saturated, which act as structure-directing and charge-balancing agents, as exemplified by $\{Ln(en)_3\}_2(\mu\text{-}OH)_2]^{4+}$ (Ln = Pr, Nd, Gd)[13b,d,e] and $[Ln_2(dien)_4(\mu\text{-}OH)_2]^{4+}$ [Ln = Eu,[13c] Y (this work)]. Therefore, the unsaturated $[Eu_2(tepa)_2(\mu_2\text{-}OH)_2]^{4+}$ complex of **4** is first observed in the lanthanide chalcogenidometalate chemistry.

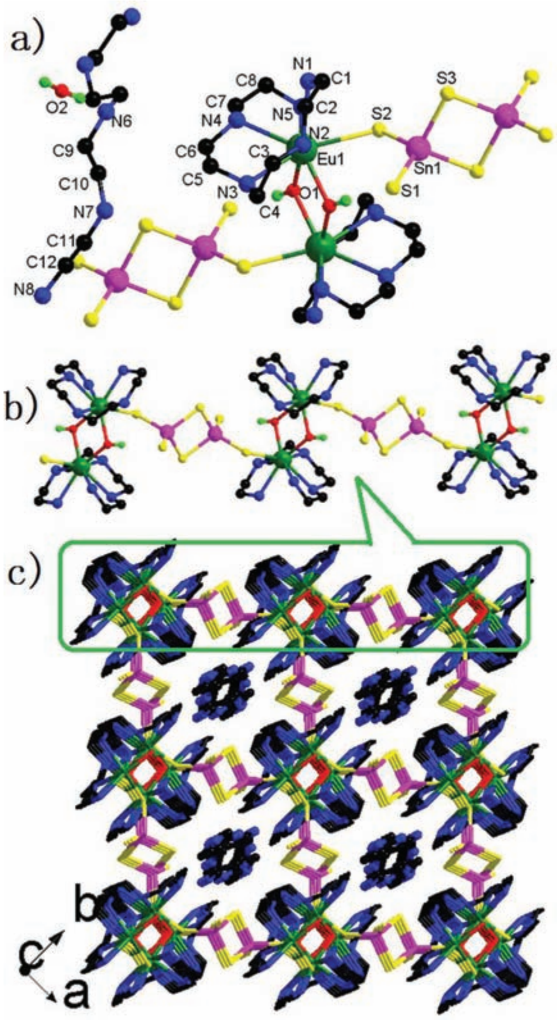

Figure 3. (a) Crystal structure of **4**. (b) 1-D $[Eu_2(tepa)_2(\mu\text{-}OH)_2(\mu\text{-}Sn_2S_6)]_n$ neutral chain. (c) 3-D supramolecular network in **4**. The H atoms bonded to C and N atoms are omitted for clarity.

The $[Sn_2S_6]^{4-}$ anion acting as a bidentate bridging ligand connects neighboring $[Eu_2(tepa)_2(\mu_2\text{-}OH)_2]^{4+}$ cations by trans terminal S atoms to form a 1-D polymeric chain of $[Eu_2(tepa)_2(\mu\text{-}OH)_2(\mu\text{-}Sn_2S_6)]_n$ (Figure 3b). There are two different directional chains in the crystal structure: one (chain "A") propagates along [110], the other (chain "B") runs along [101]. Chains "A" and "B" are arranged in a parallel manner with the same orientation to form a type of layers "A" and "B", respectively. They alternately stacked in a crossing manner to form a 3-D network with 1-D rectangular channels, which are filled by free tepa and water molecules (Figure 3c).

So far, a large number of 1-D group 13−15 chalcogenidometalate chains have been reported; their stacking modes mainly display two types (Scheme 1), namely, type I is arranged in a parallel manner, as exemplified by $K_2MnSn_2Se_6$,[30] $[(C_2H_8NO)(C_2H_8N)(CH_5N)][Sb_8S_{13}]$,[31] $[appH]_{0.5}[MS_2]$ (M = In, Ga, app = 1,4-bis(3-aminopropyl)piperazine),[32] $[M(en)_3](en)[In_2Te_4]$ (M = Ni, Co),[23b] where 1-D chains are separated from each other by either metal cations, protonated amine, or complex cations, while type II is aligned

Scheme 1. Stacking Modes of 1-D Chalcogenidometalate Chains

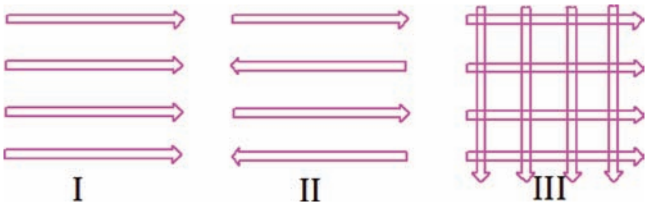

in an antiparallel fashion, such as $[\{Mn(en)_2\}_2(\mu\text{-en})(\mu\text{-}Sn_2S_6)]$,[11] $[Ln(en)_3(H_2O)_x(\mu_{3\text{-}x}\text{-}SbS_4)]$ (Ln = La, x = 0; Ln = Nd, Sm, x = 1),[29a,b] $[\{Ln(dien)_2\}_4(\mu_4\text{-}Sn_2Se_9)(\mu\text{-}Sn_2Se_6)]$ (Ln = La, Ce, Nd),[13a,b] $[Ln(dien)_2(\mu_3\text{-}AsSe_4)]$ (Ln = Nd, Sm),[29c] and $[Ce(dien)_2(\mu_3\text{-}SbS_4)]$,[29e] where inorganic−organic hybrid chain is propitious to the H-bonding interactions that play an important role in stabilizing crystal structure. Some pure inorganic chalcogenidometalate chains also adopt the antiparallel fashion, such as $[(C_6H_{16}N_2)(C_6H_{14}N_2)][Sb_6S_{10}]$,[31] $[C_8H_{22}N_2][Sb_4S_7]$,[31] $[Ni(tren)_2]_2[Ni(tren)(en)]_2(Sb_4S_8)_2\cdot 0.25H_2O$,[33] and $[Mg(en)_3][Sb_4S_7]$.[34] However, the crossing manner (type III) is very scarce; the limited examples are selenidoarsenates $[M(phen)_3][As_2Se_2(\mu\text{-}Se_3)(\mu\text{-}Se_5)]$ (M = Co, Ni),[35] where two different directional inorganic chains, $[As_2Se_2(\mu\text{-}Se_3)(\mu\text{-}Se_5)]_n$, alternately stack in a crossing manner creating pseudoparallelogram channels to accommodate the $[M(phen)_3]^{2+}$ cations, but organic−inorganic hybrid chalcogenidometalate chains adopting type III is only observed in **4**.

UV/vis, Fluorescence Spectra, and Thermogravimetric Analyses. Optical diffuse reflection spectra of **1**−**4** were measured at room temperature (Figure 4). The absorption data were calculated from the reflectance using the Kubelka−Munk function.[36] The absorption band edges at 2.40 eV for **1**, 2.48 eV for **2**, 2.76 eV for **3**, and 2.91 eV for **4** are compared with those of $[Ln_2(en)_6(\mu_2\text{-}OH)_2]Sn_2S_6$ [Ln = Nd (2.42 eV), Gd (3.17 eV)][13d] and $[Na_{10}(H_2O)_{32}][Zn_5Sn(\mu_3\text{-}S)_4(SnS_4)_4]\cdot 2H_2O$ (3.30 eV),[37] which exhibit the properties of a wide-band gap semiconductor. In addition, the weak absorptions at 2.58 and 2.66 eV in **3** presumably arise from f−f electronic transition of lanthanide complexes.

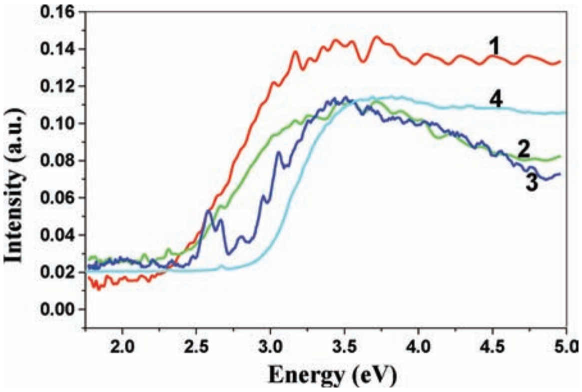

Figure 4. Diffuse reflection spectra of **1**−**4**.

The excitation spectra of **2** and **4** are shown in Supporting Information, Figure S2, monitoring emission at 617 nm. Four excitation bands, which could be assigned to the electronic transitions of the Eu^{3+} ions, $^7F_0 \rightarrow {}^5L_7$ at 386 nm, $^7F_0 \rightarrow {}^5L_6$ at 396 nm, $^5F_0 \rightarrow {}^5D_3$ at 416 nm, and $^7F_0 \rightarrow {}^5D_2$ at 463 nm are identified. Among these excitation bands, only the prominent excitation peak at 396 nm has been selected for the measurement of emission spectra of Eu^{3+} ions (Figure 5).

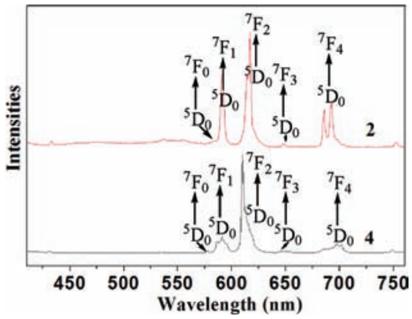

Figure 5. Emission spectra of **2** and **4** at room temperature.

The several emission bands in the range of 578−705 nm are observed by the $^5D_0 \rightarrow {}^7F_J$ (J = 0−4) transitions. Of them, the transition $^5D_0 \rightarrow {}^7F_2$ (617 nm for **2** and 610 nm for **4**) has shown a strong red emission, which is close related to Eu^{3+} center surrounded by N (or O) and S atoms in distorted monocapped square antiprism (EuN_8S) or distorted bicapped trigonal prism (EuN_5O_2S) with lower symmetries.[38] Because of the shielding effect of $4f^6$ electrons by 5s and 5p electrons in the outer shells in the Eu^{3+} ion, narrow emission bands are produced. When excited at 415 nm $[^6H_{5/2} \rightarrow (^6P_{5/2}, {}^4P_{5/2})]$, **3** displays four typical emission transitions of Sm^{3+} ion (Supporting Information, Figure S3), which are assigned to $^4G_{5/2} \rightarrow {}^6H_{5/2}$ (564 nm), $^4G_{5/2} \rightarrow {}^6H_{7/2}$ (601 nm), $^4G_{5/2} \rightarrow {}^6H_{9/2}$ (644 nm), and $^4G_{5/2} \rightarrow {}^6H_{11/2}$ (679 nm).[39] Furthermore, **2** and **4** exhibit weak emission bands at 433 and 430 nm, respectively, while **3** displays several strong emissions from 454 to 495 nm for **3**, which are probably originated from the amine ligands because similar emissions are also observed for the amine hydrochlorides.[40]

■ CONCLUSIONS

A series of new lanthanide thiostannates(IV) containing different multidentate chelating amines have been synthesized via solvothermal methods and structurally characterized. The multidentate chelating amines display a significantly structural directing effect onto the structure of lanthanide thiostannates(IV). The en[13d,e] or dien (this work) amines with smaller steric hindrance can be effectively distributed around the coordination sphere of the Ln^{3+} ion and leave limited space for other smaller μ-OH ligands to give a saturated lanthanide complex, which prevents the $[Sn_2S_6]^{4-}$ anion from further bonding to the Ln^{3+} ion. But the teta, tren, or tepa amines with larger steric hindrance can leave enough space around the coordination sphere of the Ln^{3+} ion for the $[Sn_2S_6]^{4-}$ anion to further bond to the Ln^{3+} ion. Because of the different dentate number of teta (or tren) and tepa amines, two types of unsaturated lanthanide complexes, $[Ln(teta)(tren)]^{3+}$ (Ln = Eu, Sm) and $[Eu_2(tepa)_2(\mu_2\text{-}OH)_2]^{4+}$, are formed, which result in the formation of two new types of lanthanide thiostannates(IV). Therefore, the successful synthesis of the title compounds provides possibilities of making other novel lanthanide thiostannates(IV) with structural diversity and interesting physicochemical properties by different multidentate chelating amines as the structure directing agents.

■ ASSOCIATED CONTENT

Ⓢ Supporting Information

Crystal data in CIF format, excitation and emission spectra, TG curve, 3-D H-bonding network structure of **1**, and hydrogen bonds of **1** and **2**. This material is available free of charge via the Internet at http://pubs.acs.org.

■ AUTHOR INFORMATION

Corresponding Author

*E-mail: Jianzhou888888@163.com or Jianzhou888888@yahoo.com.cn.

■ ACKNOWLEDGMENTS

This work was supported by the NNSF of China (Nos. 20961011 and 21163022), the NSF of Guangxi Province (No. 2010GXNSFB013017), the NSF of the Education Committee of Guangxi Province (No. 201012MS182), the Key Project of Chinese Ministry of Education and Program for Excellent Talents in Guangxi Higher Education Institutions. The authors are also grateful to Yulin Normal University for financial support.

■ REFERENCES

(1) (a) Zhou, J.; Dai, J.; Bian, G.; Li, C. *Coord. Chem. Rev.* **2009**, *253*, 1221−1247. (b) Kromm, A.; Almsick, T.; Sheldrick, W. S. *Z. Naturforsch.* **2010**, *65b*, 918−936. (c) Seidlhofer, B.; Pienack, N.; Bensch, W. *Z. Naturforsch.* **2010**, *65b*, 937−975. (d) Zhang, Q.; Bu, X.; Lin, Z.; Biasini, M.; Beyermann, W. P.; Feng, P. *Inorg. Chem.* **2007**, *46*, 7262−7264. (e) Xu, G.; Guo, P.; Song, S.; Zhang, H.; Wang, C. *Inorg. Chem.* **2009**, *48*, 4628−4630. (f) Schaefer, M.; Näther, C.; Lehnert, N.; Bensch, W. *Inorg. Chem.* **2004**, *43*, 2914−2921. (g) Manos, M. J.; Jang, J. I.; Ketterson, J. B.; Kanatzidis, M. G. *Chem. Commun.* **2008**, 972−974. (h) Philippidis, A.; Bakas, T.; Trikalitis, P. N. *Chem. Commun.* **2009**, 1556−1558.

(2) (a) Behrens, M.; Scherb, S.; Näther, C.; Bensch, W. *Z. Anorg. Allg. Chem.* **2003**, *629*, 1367−1373. (b) Zhou, J.; Liu, X.; Chen, G.; Zhang, F.; Li, L. *Z. Naturforsch.* **2010**, *65b*, 1229−1234. (c) Jia, D.; Dai, J.; Zhu, Q.; Zhang, Y.; Gu, X. *Polyhedron* **2004**, *23*, 937−942. (d) Jia, D.; Zhang, Y.; Dai, J.; Zhu, Q.; Gu, X. *Z. Anorg. Allg. Chem.* **2004**, *630*, 313−318. (e) Li, J.; Chen, Z.; Emge, T. J.; Yuen, T.; Proserpio, D. M. *Inorg. Chim. Acta* **1998**, *273*, 310−315. (f) Shreeve-Keyer, J. L.; Warren, C. J.; Dhingrat, S. S.; Haushalter, R. C. *Polyhedron* **1997**, *16*, 1193−1199. (g) Chen, Z.; Wang, R. *Acta Phys. Chim. Sin.* **1999**, *15*, 1070−1075. (h) Ruzin, E.; Zimmermann, C.; Hillebrecht, P.; Dehnen, S. *Z. Anorg. Allg. Chem.* **2007**, *633*, 820−829. (i) Duan, H.-B.; Hu, Z.; Jia, B.; An, Y.-L. *Acta Crystallogr.* **2006**, *E62*, m2709−m2710. (j) Fu, M.-L.; Guo, G.-C.; Liu, B.; Wu, A.-Q.; Huang, J.-S. *Chin. J. Inorg. Chem.* **2005**, *21*, 25−29.

(3) Kromm, A.; Sheldrick, W. S. *Acta Crystallogr.* **2006**, *E62*, m2767−m2769.

(4) (a) Zhou, J.; Bian, G.; Dai, J.; Zhang, Y.; Tang, A.; Zhu, Q. *Inorg. Chem.* **2007**, *46*, 1541−1543. (b) Zhou, J.; Zhang, Y.; Tang, A.; Bian, G.; Jia, D.; Dai, J. *Inorg. Chem. Commun.* **2007**, *10*, 348−351. (c) Zhang, Y.; Zhou, J.; Tang, A.; Bian, G.; Dai, J. *J. Chem. Crystallogr.* **2010**, *40*, 496−500. (d) Pienack, N.; Lehmann, S.; Lühmann, H.; El-Madani, M.; Näther, C.; Bensch, W. *Z. Anorg. Allg. Chem.* **2008**, *634*, 2323−2329.

(5) Pienack, N.; Näther, C.; Bensch, W. *Eur. J. Inorg. Chem.* **2009**, 1575−1577.

(6) Pienack, N.; Möller, K.; Näther, C.; Bensch, W. *Solid State Sci.* **2007**, *9*, 1110−1114.

(7) Pienack, N.; Puls, A.; Näther, C.; Bensch, W. *Inorg. Chem.* **2008**, 47, 9606−9611.

(8) Pienack, N.; Näther, C.; Bensch, W. *Solid State Sci.* **2007**, *9*, 100−107.

(9) Pienack, N.; Bensch, W. *Z. Anorg. Allg. Chem.* **2006**, *632*, 1733−1736.

(10) Wang, Y.; Baiyin, M.; Ji, S.; Liu, X.; An, Y.; Ning, G. *Chem. Res. Chin. Univ.* **2006**, *22*, 411−414.

(11) Gu, X.; Dai, J.; Jia, D.; Zhang, Y.; Zhu, Q. *Cryst. Growth Des.* **2005**, *5*, 1845−1848.

(12) Kromm, A.; Sheldrick, W. S. *Z. Anorg. Allg. Chem.* **2008**, *634*, 1005−1010.

(13) (a) Chen, J.; Jin, Q.; Pan, Y.; Zhang, Y.; Jia, D. *Chem. Commun.* **2009**, 7212−7214. (b) Liang, J.; Chen, J.; Zhao, J.; Pan, Y.; Zhang, Y.; Jia, D. *Dalton Trans.* **2011**, *40*, 2631−2637. (c) Zhu, A.; Jin, Q.; Jia, D.; Gu, J.; Zhang, Y. *Eur. J. Inorg. Chem.* **2008**, 4756−4761. (d) Zhao, Q.; Jia, D.; Zhang, Y.; Song, L.; Dai, J. *Inorg. Chim. Acta* **2007**, *360*, 1895−1901. (e) Jia, D.; Zhu, A.; Deng, J.; Zhang, Y. *Z. Anorg. Allg. Chem.* **2007**, *633*, 1246−1250. (f) Feng, M.; Ye, D.; Huang, X. *Inorg. Chem.* **2009**, *48*, 8060−806. (g) Chen, J.; Liang, J.; Zhao, J.; Jiang, W.; Zhang, Y.; Jia, D. *Chin. J. Struct. Chem.* **2010**, *29*, 1869−1873.

(14) (a) Chen, M.-C.; Li, L.-H.; Chen, Y.-B.; Chen, L. *J. Am. Chem. Soc.* **2011**, *133*, 4617−4624. (b) Churbanov, M. F.; Scripachev, I. V.; Shiryaev, V. S.; Plotnichenko, V. G.; Smetanin, S. V.; Kryukova, E. B.; Pyrkov, Y. N.; Galagan, B. I. *J. Non-Cryst. Solids* **2003**, *326−327*, 301−305. (c) Tonchev, D. T.; Haugen, C. J.; DeCorby, R. G.; McMullin, J. N.; Kasap, S. O. *J. Non-Cryst. Solids* **2003**, *326/327*, 364−368. (d) Wruck, D.; Klimakow, A.; Rau, B.; Henneberger, F. *Semicond. Sci. Technol.* **2001**, *16*, 885−888. (e) Schmidt, T.; Mueller, G.; Spanhel, L.; Kerkel, K.; Forchel, A. *Chem. Mater.* **1998**, *10*, 65−71. (f) Raola, O. E.; Strouse, G. F. *Nano Lett.* **2002**, *2*, 1443−1447.

(15) Volkonskaya, T. I.; Gorobets, A. G.; Kizhaev, S. A.; Smirnov, I. A.; Tikhonov, V. V.; Guittard, M.; Lavenant, C.; Flahaut, J. *Phys. Status Solidi A* **1980**, *57*, 731−734.

(16) Aitken, J. A.; Lekse, J. W.; Yao, J. L.; Quinones, R. *J. Solid State Chem.* **2009**, *182*, 141−146.

(17) Zhao, H. J.; Li, L. H.; Wu, L. M.; Chen, L. *Inorg. Chem.* **2010**, *49*, 5811−5817.

(18) Kornienko, A.; Banerjee, S.; Kumar, G. A.; Riman, R. E.; Emge, T. J.; Brennan, J. G. *J. Am. Chem. Soc.* **2005**, *127*, 14008−14014.

(19) Zhou, J.; Yin, X.; Zhang, F. *CrystEngComm* **2011**, *13*, 4806−4809.

(20) (a) Sheldrick, G. M. *SHELXS-97, Program for the Solution of Crystal Structures*; University of Göttingen: Göttingen, Germany, 1997. (b) Sheldrick, G. M. *Acta Crystallogr.* **1990**, *A46*, 467−473.

(21) (a) Sheldrick, G. M. *SHELXL-97, Program for the Refinement of Crystal Structures*; University of Göttingen: Göttingen, Germany, 1997. (b) Sheldrick, G. M. *Acta Crystallogr.* **2008**, *A64*, 112−122.

(22) Semenova, L. I.; White, A. H. *Aust. J. Chem.* **1999**, *52*, 539−550.

(23) (a) Wang, G.-M.; Sun, Y.-Q.; Yang, G.-Y. *J. Solid State Chem.* **2005**, *178*, 729−735. (b) Zhou, J.; Zhang, Y.; Bian, G.; Zhu, Q.; Li, C.; Dai, J. *Cryst. Growth Des.* **2007**, *7*, 1889−1892.

(24) (a) Demir, S.; Yilmaz, V. T.; Harrison, W. T. A. *Acta Crystallogr.* **2006**, *C62*, o216−o218. (b) Wardell, S. M. S. V.; Wardell, J. L.; Low, J. N.; Glidewell, C. *Acta Crystallogr.* **2006**, *C62*, o647−o649.

(25) (a) Lin, Z.; Zhang, J.; Zhao, J.; Zheng, S.; Pan, C.; Wang, G.; Yang, G. *Angew. Chem., Int. Ed.* **2005**, *44*, 6881−6884. (b) Wang, Y.; Yu, J.; Guo, M.; Xu, R. *Angew. Chem., Int. Ed.* **2003**, 42, 4089−4092.

(26) Melullis, M.; Brandmayer, M. K.; Dehnen, S. *Z. Anorg. Allg. Chem.* **2006**, *632*, 64−72.

(27) (a) Li, C.; Chen, X.; Zhou, J.; Zhu, Q.; Lei, Z.; Zhang, Y.; Dai, J. *Inorg. Chem.* **2008**, *47*, 8586−8588. (b) Li, C.; Zhou, J.; Zhang, Y.; Lei, Z.; Bian, G.; Dai, J. *Z. Anorg. Allg. Chem.* **2009**, *635*, 151−155.

(28) Quiroga-González, E.; Näther, C.; Bensch, W. *Solid State Sci.* **2010**, *12*, 1235−1241.

(29) (a) Jia, D.; Zhu, Q.; Dai, J.; Lu, W.; Guo, W. *Inorg. Chem.* **2005**, *44*, 819−821. (b) Jia, D.; Zhao, Q.; Zhang, Y.; Dai, J.; Zuo, J. *Inorg. Chem.* **2005**, *44*, 8861−8867. (c) Jia, D.; Zhu, A.; Deng, J.; Zhang, Y.; Dai, J. *Dalton Trans.* **2007**, 2083−2086. (d) Wang, J.; Pan, Y.; Chen, J.; Gu, J.; Zhang, Y.; Jia, D. *Dalton Trans.* **2010**, *39*, 7066−7072. (e) Lichte, J.; Näther, C.; Bensch, W. *Z. Anorg. Allg. Chem.* **2010**, *636*, 108−113.

(30) Chen, X.; Huang, X.; Fu, A.; Li, J.; Zhang, L.; Guo, H. *Chem. Mater.* **2000**, *12*, 2385−2391.
(31) Seidlhofer, B.; Spetzler, V.; Quiroga-Gonzalez, E.; Näther, C.; Bensch, W. *Z. Anorg. Allg. Chem.* **2011**, *637*, 1295−1303.
(32) Vaqueiro, P. *J. Solid State Chem.* **2006**, *179*, 302−307.
(33) Lühmann, H.; Näther, C.; Bensch, W. *Z. Anorg. Allg. Chem.* **2011**, *637*, 1007−1012.
(34) Quiroga-González, E.; Näther, C.; Bensch, W. *Z. Naturforsch.* **2009**, *64b*, 1312−1318.
(35) (a) Zhao, J.; Liang, J.; Chen, J.; Pan, Y.; Zhang, Y.; Jia, D. *Inorg. Chem.* **2011**, *50*, 2288−2293. (b) Jia, D.; Zhao, J.; Pan, Y.; Tang, W.; Wu, B.; Zhang, Y. *Inorg. Chem.* **2011**, *50*, 7195−7201.
(36) Wendlandt, W. W.; Hecht, H. G. *Reflectance Spectroscopy*; Interscience Publishers: New York, 1966.
(37) Liao, J.; Varotsis, C.; Kanatzidis, M. G. *Inorg. Chem.* **1993**, *32*, 2453−2462.
(38) (a) Weibel, N.; Charbonnière, L. J.; Guardigli, M.; Roda, A.; Ziessel, R. *J. Am. Chem. Soc.* **2004**, *126*, 4888−4896. (b) Kam, C. H.; Buddhudu, S. *Phys. B* **2004**, *344*, 182−189. (c) Lakshminarayana, G.; Qiu, J. *J. Alloys Compd.* **2009**, *476*, 720−727.
(39) (a) Lakshminarayana, G.; Buddhudu, S. *Phys. B* **2006**, *373*, 100−106. (b) Thulasiramudu, A.; Buddhudu, S. *Spectrochim. Acta , Part A* **2007**, *67*, 802−807. (c) Praveena, R.; Venkatramu, V.; Babu, P.; Jayasankar, C. K. *Phys. B* **2008**, *403*, 3527−3534. (d) Lakshminarayana, G.; Qiu, J. *Phys. B* **2009**, *404*, 1169−1180.
(40) (a) Liu, G.; Guo, G.; Wang, M.; Cai, L.; Huang, J. *J. Mol. Struct.* **2010**, *983*, 104−111. (b) Fu, M.; Guo, G.; Liu, X.; Liu, B.; Cai, L.; Huang, J. *Inorg. Chem. Commun.* **2005**, *8*, 18−21.